

Conventional Superconductivity properties of the ternary boron-nitride Nb₂BN

O. V. Cigarroa¹, S. T. Renosto¹, A. J. S. Machado¹

¹Escola de Engenharia de Lorena, Universidade de São Paulo, P.O. Box 116, Lorena - SP, Brasil;*

(Dated: November 10, 2018)

Superconducting bulk properties of ternary Nb₂BN are confirmed and are described by means of magnetization, electronic transport and specific-heat measurements. BCS conventional superconductivity is found with $T_c = 4.4$ K. Critical fields $H_{c1}(0) = 93$ Oe and $H_{c2}(0) = 2082$ Oe are extrapolated by magnetic and resistivity measurements. The specific heat data reveals $\gamma = 6.3$ mJ/mol K² and $\beta = 0.293$ mJ/mol K⁴ in good agreement with the BCS Theory.

PACS numbers: 74.20.Fg, 71.28.+d, 72.80.-r

I. INTRODUCTION

Among the known ternary carbides, Mo₂BC deserves attention due its superconducting behaviour with a T_c ranging from 5 to 7.5 K^{1,2}. Mo₂BC has an orthorhombic symmetry³ (no. 63, space group cmcm) with $a = 3.086$, $b = 17.35$ and $c = 3.047$ Å. Fig. 1 illustrates such structure, where distorted Mo₆ octahedron layers are separated from each others by zig-zag B chains which pass through the trigonal prisms of Mo atoms⁴. Carbon atoms are located at the center of the Mo octahedrons^{5,6}. Several efforts⁶⁻⁹ were made to enhance the superconducting properties of this compound by inducing chemical pressure with transition elements as $M = \text{Zr, Rh, Nb, Hf, Ta and W}$ at the Mo sites. While T_c of Mo_{2-x}M_xBC decreased with increase of x for all the alloys, only the Rh-containing alloy⁹ showed an increase up to $T_c = 9$ K.

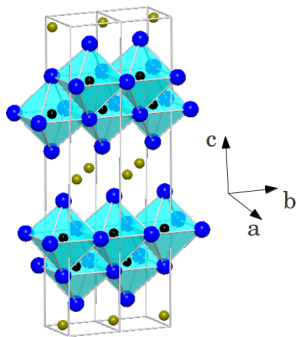


FIG. 1: Schematics of the Mo₂BC orthorhombic (cmcm) type structure. Distorted Mo₆ octahedron layers (blue spheres) with C atoms (black spheres) on their center are separated by B zig-zag chains (green spheres) at the middle of the cell unit.

After the discovery of Mo₂BC a boron-nitride with nominal Nb₂BN composition was synthesized for the first time¹⁰ as a thermodynamically stable compound at 1200°C. In this compound Nb atoms are arranged in similar distorted octahedron and are separated by B zig-zag chains as in Mo₂BC and N atoms occupy the same position as C atoms. Lattice Parameters of Nb₂BN are quite similar to those of Mo₂BC being $a = 3.17$, $b = 17.85$ and $c = 3.11$ Å. Superconductivity with critical temper-

ature close to 2.2 K was reported in Nb₂BN_x (x undetermined) compound. However other properties such as specific heat or resistivity were not performed by the authors in order to confirm bulk superconductivity. In this context our results show unambiguously bulk superconductivity at 4.4 K in single phase polycrystalline samples of Nb₂BN.

II. EXPERIMENTAL

Polycrystalline Nb₂BN samples were synthesized by conventional powder solid state reaction method. High purity 300 mesh Nb (99.99) and hexagonal BN (99.999) were used. To ensure the good quality of the primary reaction BN was degassed at 1000°C in vacuum for twenty four hours before its usage. Stoichiometric amounts (Nb 2:1 BN) of the reagents were weighted, mixed on an agatar mortar and pressed (4 tons) into pellets of cylindrical shape. Compressed mixtures were sealed on quartz tubes under 1 bar argon atmosphere and heated at 1200°C. Each 7 days of annealing the samples were quenched, grounded, pressed and encapsulated again to be treated at 1200°C. A complete reaction was obtained only after 28 days of annealing.

X-ray diffraction patterns were collected with a Panalitical Empryean X-ray diffractometer using CuK_α radiation. Rietveld refinements¹¹ were calculated using the Fullprof suite considering a error $\chi^2 \leq 2$ as the minimum standard. Magnetic, electric, and thermal, initial characterizations were made using a Quantum Design PPMS Evercool II. Magnetization (M) measurements were obtained using a commercial VSM magnetometer (Quantum Design) in a DC external field of 50 Oe in zero field cooling (ZFC) and field cooling (FC) conditions, on a temperature range (T) from 2 to 20 K. Magnetization (M) versus applied field (H) data were acquired at constant temperatures between 2 and 5 K. Electrical resistivity measurements were performed between 1.8 and 300 K using the conventional four-point method. Thin Cu wires were welded to a regular shape sample and served as the voltage and current leads, using a high purity Ag epoxy. Applied magnetic fields were also used to estimate the upper critical field. The superconducting critical temperature (T_c) was defined as the transition midpoint. The heat capacity measurements were determined using the

relaxation method of a piece cut from the sample on a calorimetric probe coupled to the PPMS system on a temperature range from 2 to 10 K.

III. RESULTS AND DISCUSSION

Figure 2 shows the diffraction pattern of a typical Nb₂BN sample after 28 days of heat treatment. All reflections can be indexed with the orthorhombic Mo₂BC structure with space group *cmcm* and without any trace of secondary phases within the limits of this technique. Rietveld refinements led to the following occupancies: Nb-1 atoms occupy the $4c$ (0, 0.721, 0.25), Nb-2 atoms occupy the $4c$ (0, 0.3139, 0), N atoms occupy the $4c$ (0, 0.192, 0) and B atoms the $4c$ (0, 0.4731, 0.25) positions. These results are in good agreement with the ones reported earlier¹⁰. The Nb-1 bonding distance have a slightly difference (2.22 and 3.01 Å) with the original Mo-1 bonding distance (2.11 and 3.086 Å) in Mo₂BC.

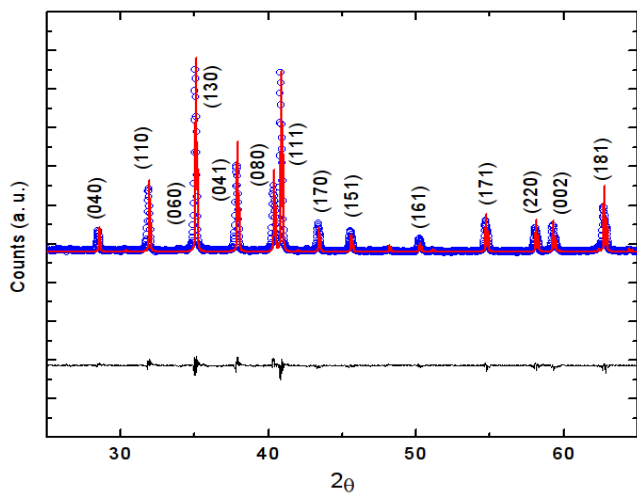


FIG. 2: X-ray diffraction pattern for polycrystalline Nb₂BN. Experimental pattern (blue dots) is compared with the simulated diffraction pattern (red line) and the difference between them (black line) as calculated in the Rietveld refinement.

The temperature dependence of the magnetization in zero-field cooled (ZFC) and field cooled (FC) conditions was measured using an applied magnetic field of 50 Oe and is presented in Figure 3. In both ZFC and FC a clear superconducting transition can be seen around 4.4 K. The superconducting volume fraction ($\sim 60\%$) can be estimated within the Meissner state through the dependence of M vs H , since the value of the superconducting state susceptibility (perfect diamagnetism) is $-1/4\pi$, according to the CGS system. Note that even without considering the demagnetization size susceptibility factor, this result suggests bulk superconductivity. On the FC curve, the flux expulsion of about 7% indicates a strong flux pinning as expected. Inset of Figure 3 displays the isothermal M versus H at $T = 2$ K that shows a type II superconductivity behaviour.

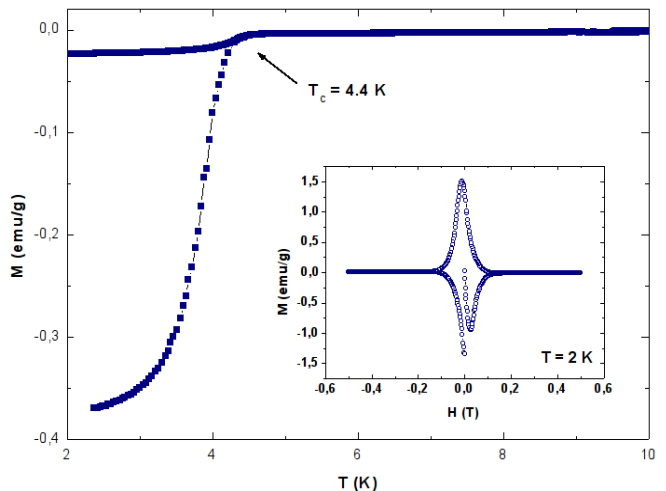


FIG. 3: Magnetization as a function of the temperature on a 50 Oe applied field of a polycrystalline Nb₂BN sample. On the inset isothermal Magnetization as a function of applied field in $T = 2$ K showing a type II superconducting behaviour.

The typical temperature dependence of the resistivity of Nb₂BN is shown in Figure 4. A sharp resistivity transition close to 4.4 K (at $\rho = 0$, $\Delta T_c \sim 0.1$ K) is clearly observed at zero applied magnetic field which indicates the high quality of the obtained samples. These results are consistent with those obtained in magnetization measurements. The inset in Fig. 4 shows the resistivity dependence on the applied magnetic field. An estimate of the upper critical field at 0 K [$\mu_0 H_{c2}(0)$] can be made through the Werthamer, Helfand, and Hohenberg (WHH) theory¹² represented by Eq. 1. According to this theory $\mu_0 H_{c2}(0)$ can be estimated inside the limit of a short electronic mean-free path (dirty limit) and is given by :

$$\mu_0 H_{c2}(0) = -0.693 T_c (dH_{c2}/dT)_{T=T_c} \quad (1)$$

The temperature dependence of $\mu_0 H_{c2}(T)$ is shown in Figure 5 where the black line represents the conventional fitting of $\mu_0 H_{c2}(0)$ obtained using the Eq. 1. The critical field $H_{c2}(0)$ is estimated to be ~ 2082 Oe, a value that suggests a type II superconductivity. Another estimate of $H_{c2}(0)$ was obtained by using the data of magnetization versus applied field on different temperatures as shown on Figure 6. The followed criterion consisted of taking the corresponding field of $H_{c2}(T) = 0$ for the given temperature, plotting and fitting the values with the equation 1 to obtain $H_{c2}(0)$. The result is completely consistent with the resistivity method. The lower critical field ($H_{c1}(0)$) was extrapolated from the applied magnetic field dependence of the magnetization at several temperatures shown in Figure 6a, using the Ginzburg-Landau equation¹³ $H_{c1}(T) = H_{c1}(0)(1 - (T/T_c)^2)$ which gives $H_{c1}(0) \sim 93$ Oe. The values of H_{c1} were determined by examining the divergence from linearity of the slope

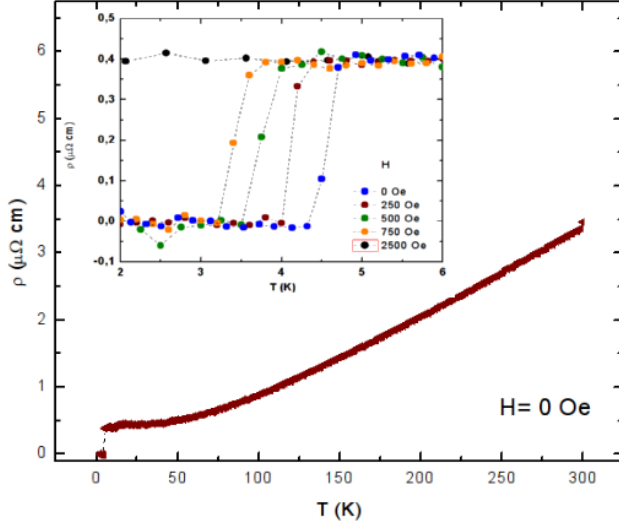


FIG. 4: Electrical resistivity (ρ) versus temperature of Nb_2BN from 2 to 300 K displaying the characteristic superconducting transition at 4.4 K. Inset shows the evolution of T_c with different applied fields.

of the magnetization curve (Fig. 6b), using the criterion $\Delta M = 10^{-3}$ emu for the difference between the Meissner line and magnetization signal. The calculated values of $H_{c1}(0)$ and $H_{c2}(0)$ allows us to estimate the coherence length and penetration deep through of the Ginzburg-Landau (GL) formulas¹³:

$$\mu_0 H_{c1}(0) = \frac{\phi_0}{2\pi\lambda_0^2} \quad (2)$$

$$\mu_0 H_{c2}(0) = \frac{\phi_0}{2\pi\xi_0^2} \quad (3)$$

where ϕ_0 is a quantum flux equal $2.068 \times 10^{-15} \text{ T}\cdot\text{m}^{-2}$, which yields $\xi_0 \sim 425 \text{ \AA}$ and $\lambda_0 \sim 188 \text{ nm}$ at 0 K. Using the relation $\kappa_{GL} = \lambda_0/\xi_0$ we obtained the value $\kappa_{GL} = 4.42$ that agrees with the previous results indicating a type-II superconducting behaviour.

While the magnetization and resistivity suggest bulk superconductivity in Nb_2BN , an anomaly in the specific heat measurement is necessary for confirmation. Figure 7 displays the specific heat divided by temperature (C/T) versus T^2 at zero applied magnetic field. A jump in the specific heat is clearly observed on the midpoint of the transition at $T_c = 4.4 \text{ K}$ and a small transition length of only $\Delta T_c \sim 0.3 \text{ K}$. The consistency between the magnetization, resistivity, and heat capacity transitions is a clear evidence of bulk superconductivity in Nb_2BN . The normal state specific heat (C_n) is assumed to have contributions from the standard linear electronic contribution (γT) term and the cubic phonon (βT^3) term.

In Figure 7 the normal state specific heat (C_n) can be fitted to the expression $C_n = \gamma T + \beta T^3$ by a least squares

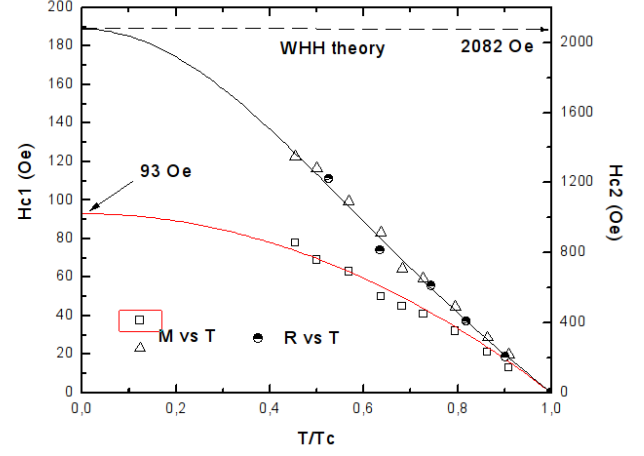


FIG. 5: The temperature dependence of H_{c2} and H_{c1} of Nb_2BN . Experimental points taken from M vs H and R vs T are marked as dots. The red line represents the GL fit for $H_{c1}(T)$ and the black line corresponds to the WHH fit for $H_{c2}(T)$.

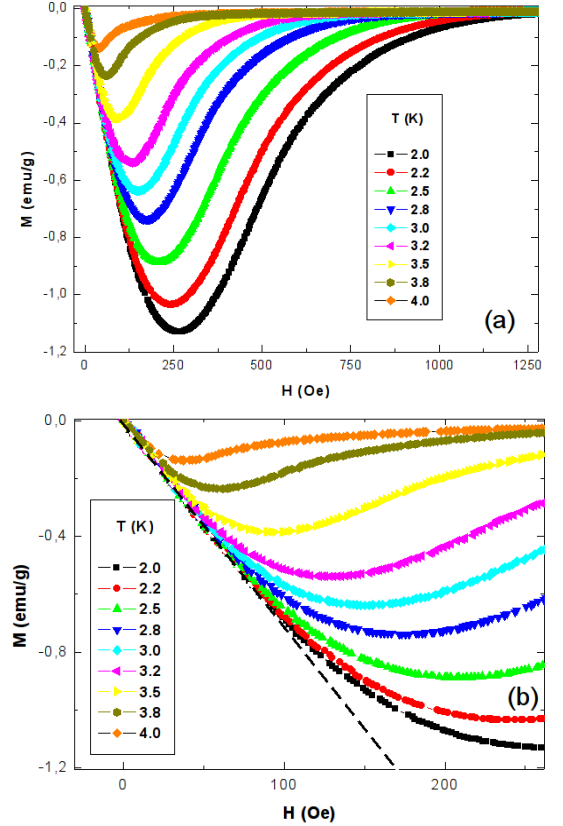


FIG. 6: Magnetization versus applied field taken at constant temperatures from 2 to 4 K. The dashed line illustrates the criterion used to determine the difference between M and the linear behaviour below H_{c1} .

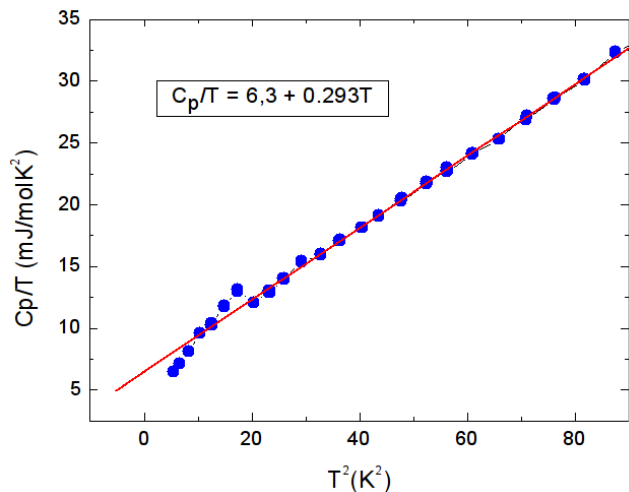


FIG. 7: C_p/T vs T^2 curve at zero magnetic field shows the superconducting critical temperature close to 4.4 K, which is consistent with the electrical transport and magnetization measurements. The solid red line is the fit of the experimental data to $c = \gamma T + \beta T^3$ between 2 and 30.0 K.

analysis, with resultant values of $\gamma = 6.3$ mJ/mol K² and $\beta = 0.293$ mJ/mol K⁴. The β value corresponds to a Debye temperature of $\Theta_D \sim 298$ K. The Sommerfeld coefficient γ suggests a moderated density of states at the Fermi level typical of other transition-metal superconductors.

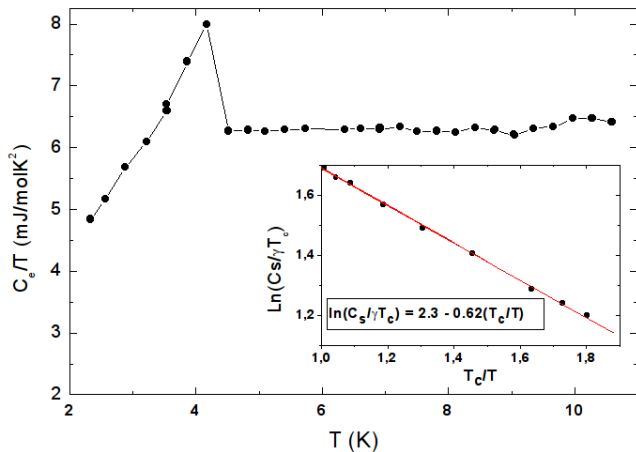


FIG. 8: Temperature dependence of the electronic specific-heat divided by the temperature (C_e/T). The inset shows the linear fitting of the $\ln(C_s/\gamma T_c)$ against T_c/T .

A subtraction of the phonon contribution from the total specific heat allows the analysis of just the electronic contribution (C_e), displayed here as C_e/T versus T in Figure 8. The analysis of the specific heat anomaly shows the magnitude of the jump at T_c to be $\Delta C_e/T_c \sim 0.88$,

which is significantly smaller than the weak-coupling BCS limit of 1.43. However, this apparent inconsistency is related with the superconducting fraction estimated from magnetization measurement displayed in Fig. 3. Although the reason for the estimated value from specific heat measurement diverges from BCS prediction is not obvious, the size of the jump strongly suggests that the superconducting behaviour is in a BCS weak coupling limit. Indeed, the exponential behaviour of the electronic component on the superconducting state is in good agreement with the BCS theory as shown in inset of Figure 8. The linear behaviour of the logarithmic scale versus T_c/T is totally consistent with BCS prediction of the superconducting state below T_c . The comparison with BCS formula for C_e below T_c :

$$\frac{C_e}{\gamma T_c} = 8.5e^{\frac{0.82\Delta(0)}{K_B T}} \quad (4)$$

which yields an energy gap (Δ_0) of 0.65 meV for $T \rightarrow 0$ and $2\Delta_0/K_B T_c = 3.45$ which again is a signal of a weak BCS coupling value. Then, all results from specific heat suggest that Nb₂BN is a conventional BCS superconducting material. In all BCS superconductors the Cooper-pairing is phonon mediated and the dimensionless electron-phonon constant λ can be determined by the McMillan equation¹⁴:

$$T_c = \frac{\theta_D}{1.45} \exp\left\{\frac{-1.04(1 + \lambda)}{\lambda - \mu^*(1 + 0.62\lambda)}\right\} \quad (5)$$

If the Coulomb coupling constant μ^* is considered to be 0.13, which is a usual value, and the Debye temperature from specific-heat is considered 298 K, the value $\lambda \sim 0.62$ the obtained value is again in excellent agreement with a weak coupling BCS value for other conventional superconducting materials¹⁵.

IV. CONCLUSIONS

In this paper the superconducting properties of Nb₂BN were explored. Conventional bulk superconductivity was found at $T_c = 4.4$ K with superconducting critical fields $H_{c1}(0) = 93$ and $H_{c2}(0) = 2082$ Oe. Results suggest a conventional type II superconductivity with $\kappa_{GL} = 4.42$ and bulk superconductivity was confirmed through specific heat measurements, showing the values of $\gamma = 6.3$ mJ/mol K² and $\beta = 0.293$ mJ/mol K⁴ in good agreement with the BCS Theory.

ACKNOWLEDGEMENTS

This work was financed by the Brazilian agency CNPq 302892/2011-7, 140804/2012-9 and FAPESP 2010/11770-3

* Electronic address: orlandocv@usp.br

- ¹ L. E. Toth., *J. Less-Common Metals*, **13**, 129 (1967).
- ² L. E. Toth and J. Zbasnik, *Acta Met.*, **16**, 1177 (1968).
- ³ L. E. Toth, *Transition Metal Carbides and Nitrides*, **59**, (1971).
- ⁴ W. Jeitschko, H. Novotny and F. Benesovsky, *Monatsh. Chem.*, **3**, 565 (1963).
- ⁵ J. O. Bovin, M. O'Keeffe and L. Stenberg, *J. Solid State Chem.*, **22**, 221 (1977).
- ⁶ S. Gordon, A. G. Tharp and Q. Johnson, *Acta Crystallogr.*, **25**, 698 (1969).
- ⁷ V. Sadagopan and H. Gatos, *J. Phys. Chem. Solids*, **27**, 235 (1966).
- ⁸ E. Rudy, F. Benesovsky and L. Toth, *Z. Metallk.*, **54**, 345 (1963).
- ⁹ P. Lejay, B. Chevalier, J. Etourneau and P. Hagenmuller, *J. Less-Common Met.*, **14**, 34 (1968).
- ¹⁰ P. Rogl G., *Phase diagrams of ternary metal-boron-carbon systems*, **MSIT-ASM International**, 261 (1998).
- ¹¹ Young, R. A., *The Rietveld Method*, International Union of Crystallography, Oxford University Press, New York (1993).
- ¹² C. K. Poole, H. A. Farach, R. J. Creswic, *Handbook of Superconductivity*, **305** (1999).
- ¹³ Kittel, C., *Introduction to Solid State Physics*, 6th ed., John Wiley & Sons, inc., New York (1993).
- ¹⁴ W.L. McMillan, *Phys. Rev. B*, textbf167, 331 (1968).
- ¹⁵ P. Roedhammer, E. Gmlin, W. Weber and J.P. Remeika, *Phys. Rev. B*, **15** (1977).